Solvent-Induced Phase Separation in Colloidal Fluids

Hartmut Löwen

Sektion Physik der Universität München, Theresienstrasse 37, 80333 München, Germany

(Received 16 September 1994)

The phase behavior of a colloidal fluid near a solvent first-order phase transition is investigated. Based on analysis and computer simulation of a Ginzburg-Landau model for the solvent coupled to the colloidal coordinates, two scenarios of phase separation are predicted, induced by wetting of the colloidal surfaces with one solvent phase. Phase separation either starts spontaneously from a homogeneous colloidal phase with a one-phase solvent or from nonpercolating clusters of the wetting solvent phase which on average contain few colloidal particles.

PACS numbers: 82.70.Dd, 61.20.–p, 64.70.–p

Since the previous century [1,2] it is well known that macromolecular particles in a two-phase medium exhibit different concentrations in the two solvent phases. This spontaneous partitioning is energetically driven by a different macroparticle surface tension in the two solvent phases. Many examples of such demixing phenomena have been found during the past decades, for a review, see Refs. [3]. Systematic experiments by Beysens and coworkers [4] and by Gallagher and Maher [5] on colloidal particles embedded in a near-critical solvent mixture of 2,6-lutidine plus water have revealed that the phase separation can be viewed as reversible flocculation and is hence different from colloidal coagulation due to the van der Waals attraction [6].

Theoretical work of colloidal partitioning or flocculation in a two-phase solvent is still rather rudimentary; it has either focused on a phenomenological thermodynamic treatment [2] or on general arguments [7] known from wetting or capillary condensation [8] in a simple fixed geometry of two spheres. The essential point which is neglected in any of these arguments, however, is that the colloidal particles are interacting via their direct forces *and* the indirect interaction mediated by the surface free energy of the solvent phases. The latter interaction is dictated by wetting properties in a complicated geometry made up by an ensemble of spheres and therefore clearly has a *many-body* character.

The aim of this Letter is to propose and discuss a general model which includes this effect systematically and contains parameters whose relation to microscopic quantities is known. Basically it consists of a Ginzburg-Landau approach for the first-order solvent phase transition, coupled to the colloidal coordinates and combined with the direct forces between the colloidal particles. An analysis of this model predicts a rich scenario of solvent-induced colloidal phase separation: There are two different colloidal one-phase regions, both of them are fluidlike. The first corresponds to the ordinary fluid phase in a one-phase solvent while the second contains nonpercolating clusters of the solvent phase preferred by the colloidal surface. This second situation is stable when the clusters contain few colloidal particles on average. From both situations phase separation occurs in two homogeneous colloidal fluid phases with different particle densities both of which involve a one-phase solvent. Similar solvent-induced phase transitions have been suggested for polymers in near-critical solvents, see, e.g., Ref. [9].

In the Ginzburg-Landau approach we are adopting, the first-order phase transition of the solvent is modeled by a dimensionless scalar order parameter field $\phi(\mathbf{r})$ [10]. The order parameter ϕ stands for the relative density difference between the two coexisting phases if a liquid-gas, freezing, or A-rich to B-rich solvent transition is considered. For a liquid-crystalline solvent near the isotropic-nematic transition, ϕ is the mean-squared orientation, and for magnetic solvents ϕ equals the mean-squared magnetization of the two solvent phases. Consequently, quite a number of different physical situations can be captured within the Ginzburg-Landau description. Without loss of generality ϕ can be scaled to be 1 in the first and -1 in the other solvent phase. Then, in the absence of any colloidal particles, the associated free energy $\mathcal{F}_0$ of the solvent in a volume Ω is a functional of $\phi(\mathbf{r})$:

$$\mathcal{F}_0[\phi(\mathbf{r})] = \int_\Omega d^3r\{\tfrac{1}{2} f_0 \xi^2 [\nabla\phi(\mathbf{r})]^2 + f(\phi(\mathbf{r}))\}. \quad (1)$$

Here, the square-gradient term describes a free energy penalty of an inhomogeneous system, resulting in a surface tension $\gamma > 0$ between the two solvent phases. Microscopically ξ is the correlation length of order parameter fluctuations and f_0 a free energy density scale. For the local free energy density $f(\phi)$, the Ginzburg-Landau form $f(\phi) = f_0(\phi^4 - 2\phi^2 + 4\epsilon\phi)$ is taken. For $\epsilon = 0$, $f(\phi)$ has a double-well structure with minima at $\phi = \pm 1$, corresponding to two coexisting solvent phases with a planar surface tension $\gamma = 4\sqrt{2} f_0 \xi/3$. For $\epsilon \neq 0$, an off-coexistence situation is described. The difference in free energy density between the two phases is $8 f_0 \epsilon$, hence ϵ measures the distance from coexistence. The free energy density $f(\phi)$ can be linked to microscopic quantities using, e.g., density functional theory [10].

 0031-9007/95/74(6)/1028(4)$06.00

In addition, we are considering N colloidal particles in a volume Ω with a particle number density $\rho = N/\Omega$ at fixed given temperature T. One configuration is characterized by the positions $\{\mathbf{R}_i, i = 1, \ldots, N\}$. The particles interact via direct repulsive forces stemming from a pairwise potential $V_{\rm pp}(r)$, where r is the interparticle separation. Depending on the kind of colloid, $V_{\rm pp}(r)$ can be a hard-sphere, soft-sphere, or screened Coulomb potential [6]. Next, the free energy resulting from the coupling between $\phi(\mathbf{r})$ and the colloidal coordinates is modeled by

$$\mathcal{F}_{\rm po}([\phi(\mathbf{r})],\{\mathbf{R}_i\}) = \int_\Omega d^3r\, \phi(\mathbf{r}) \sum_{i=1}^{N} V_{\rm po}(|\mathbf{R}_i - \mathbf{r}|), \quad (2)$$

where $V_{\rm po}(r)$ contains microscopic information about the wetting properties of the colloidal surface; for instance, the phase belonging to negative ϕ is favored if $V_{\rm po}$ is positive at the particle radius.

Treating the solvent phase transition in mean-field fashion, our model is finally defined by the total Lagrangian:

$$\mathcal{L} = \sum_{i=1}^{N} \frac{M}{2}\dot{\mathbf{R}}_i^2 - \sum_{i,j=1;i<j}^{N} V_{\rm pp}(|\mathbf{R}_i - \mathbf{R}_j|) - \mathcal{F}_0[\phi(\mathbf{r})] - \mathcal{F}_{\rm po}([\phi(\mathbf{r})],\{\mathbf{R}_i\}), \quad (3)$$

where M is the macroparticle mass [11] and the dot means a time derivative. By solving the Euler equations of motion corresponding to $\{\mathbf{R}_i\}$ and $\phi(\mathbf{r})$ for sufficiently long times, one can, at least in principle, generate a large number of typical configurations in order to perform static canonical averages and calculate the phase behavior. The dynamics defined by the Lagrangian are not the real dynamics of the system but rather serve to generate typical configurations. The Euler equation for $\phi(\mathbf{r})$ is a minimization of the functional $\mathcal{F}_0 + \mathcal{F}_{\rm po}$ with respect to $\phi(\mathbf{r})$, resulting in the equilibrium order parameter profile which depends parametrically on the colloidal coordinates. The Euler equations for $\{\mathbf{R}_i\}$, in turn, involve this equilibrium order parameter profile implying that many-body forces govern the equations of motion. One therefore has to resort to further approximations keeping the analysis simple or to a numerical treatment within a computer simulation. We have followed both lines. Let us first invoke two additional approximations: (i) We assume that the order parameter field is either 1 or -1 with an infinitely thin ("sharp-kink") interface between the two solvent phases. (ii) The topology of the region occupied by the wetting solvent phase is simple. Then the phase behavior can be calculated analytically giving a general insight into the different scenarios of possible phase separation.

Performing this approximative analysis the solvent phase corresponding to a negative order parameter is called A, the other one is B. Without loss of generality we consider an off-coexistence situation with $\epsilon \geq 0$, where a fraction Ω_A/Ω of the total volume is occupied by phase A wetting the colloidal surfaces. We distinguish between two different situations: (a) The colloidal particles are covered by nonoverlapping spherical drops of phase A. (b) N_A colloidal particles are in a large region of phase A and $N - N_A$ are in that of phase B. Of course, there are two special one-phase cases of (b) where the whole space is filled either by phase B ($N_A = 0$) or by phase A ($N_A = N$), which we call (c) and (d). All situations (a)–(d) are visualized in Fig. 1.

In situation (a), the free energy of the total system is

$$F^{(a)} = 8f_0\epsilon\Omega_A + \Omega f_p(\rho,T) + N\gamma 4\pi R^2 + Nf_c^{(a)}. \quad (4)$$

Here $8f_0\epsilon\Omega_A$ is the free energy cost to create a volume Ω_A of phase A, $f_p(\rho,T)$ is the bulk free energy density of a fluid interacting via the pair potential $V_{\rm pp}(r)$ known from liquid state theory [12], and the third term describes the total surface tension between the two solvent phases, $R = (3\Omega_A/4\pi\rho\Omega)^{1/3}$, denoting the droplet radius. Finally the energy gain by wetting is approximately contained in the coupling term $f_c^{(a)} = 4\pi\int_0^\infty dr\, r^2[\Theta(R - r) - \Theta(r - R)]V_{\rm po}(r)$, where $\Theta(x)$ is the unit step function. In situation (b), on the other hand, the total free energy is

$$F^{(b)} = 8f_0\epsilon\Omega_A + \Omega_A f_p\left(\frac{N_A}{\Omega_A}, T\right) + (\Omega - \Omega_A) f_p\left(\frac{N - N_A}{\Omega - \Omega_A}, T\right) + (2N_A - N) f_c^{(b)}, \quad (5)$$

where now $f_c^{(b)} = 4\pi\int_0^\infty dr\, r^2 V_{\rm po}(r)$.

The physically realized situation is that with minimal free energy. $F^{(a)}$ has to be minimized with respect to Ω_A ($0 \leq \Omega_A \leq \Omega$) and $F^{(b)}$ with respect to Ω_A and N_A ($0 \leq N_A \leq N$). The lowest value of $F^{(a)}$ and $F^{(b)}$ corresponds to the physically realized energy and hence the complete phase behavior together with the corresponding partial densities $\rho_A = N_A/\Omega_A$ and $\rho_B = (N - N_A)/(\Omega - \Omega_A)$ is directly obtained.

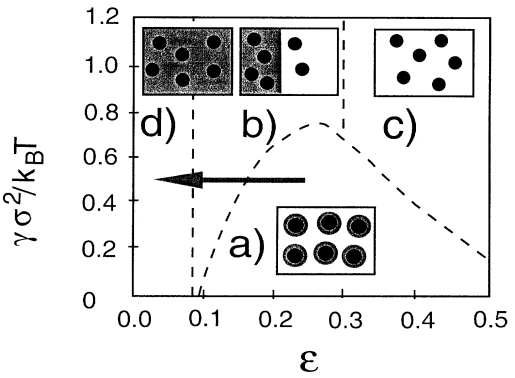

FIG. 1. Region of stability of the situations (a)–(d) in $\epsilon\gamma$ plane separated by the dashed lines as obtained within the approximate analysis. The parameters are $\rho = 0.382\sigma^{-3}$, $G = 10$, $f_0 = 2k_BT/\sigma^3$, $E = 30$, and $\alpha = 11.1$. The arrow corresponds to the path shown in Fig. 3. The colloid positions (black circles) and the grey region of phase A are schematically given in each situation.

We have also performed extensive molecular dynamics simulations solving the Euler equations of the Lagrangian $\mathcal{L}$ by using a classical version of the Car-Parrinello *ab initio* method [13] similar to the work in Ref. [14]. $N = 108$ colloidal particles were taken in a cubic box with periodic boundary conditions. The order parameter field was resolved in real space on a 64^3 cubic grid. After a long equilibration from a randomly chosen initial configuration for the colloidal particles, a typical configuration was gathered to take canonical averages. A phase separation was detected by monitoring the positions of the colloidal particles and the interface between the two solvent phases. Target quantities were the partial densities ρ_A and ρ_B and topological properties of the interface between the two solvent phases defined via $\phi(\mathbf{r}) = 0$. A convenient topological quantity is the averaged number of colloidal particles per cluster of phase A, or its inverse n_c, the averaged number of clusters per particle. If n_c vanishes, the region covered by phase A is percolating.

In our calculations, the interparticle potential was $V_{\mathrm{pp}}(r) = Gk_BT(\sigma/r)^{12}$, where G is a dimensionless amplitude and the soft-sphere diameter σ sets the length scale. In this case, explicit expressions for $f_p(\rho, T)$ were given by Hansen [15]. Furthermore, we take $V_{\mathrm{po}}(r) = -Ek_BT\sigma^{-3}\exp[-\alpha(r/\sigma)^2]$ with two dimensionless parameters $E > 0$ and α. The stability of the four situations (a)–(d), as obtained within the approximate analysis, is shown in Fig. 1 as a function of ϵ and γ. Any situation can be stable; the transition between different situations is first order as indicated by the dashed lines in Fig. 1. Phase separation [situation (b)] can be started from all one-phase situations. In an experiment, one typically varies ϵ by changing the solvent while γ and all other parameters are slowly varying. Along such an experimental path ($\gamma \approx 0.7$) with decreasing ϵ, there is phase separation from (c) to (b), then the clustered situation (a) is stable and finally phase separation is *reentering*. Typical configurations of the colloidal positions and the solvent AB interface as obtained from the computer simulations are shown in Fig. 2, both for a clustered situation [Fig. 2(a)] and complete partitioning [Fig. 2(b)]. One clearly sees that the topology of the clusters is much more complicated than assumed in the approximative analysis since clusters can fuse to contain more than one colloidal particle. In Fig. 3, for fixed γ and varying ϵ, computer simulation results from eight different runs are shown near the (a) to (b) and (b) to (d) transitions corresponding to the arrow in Fig. 1. In the clustered situation, n_c is significantly smaller than 1 and discontinuously jumps from a finite value to zero as ϵ is decreased. This shows that phase separation is directly connected to a first-order *percolation transition* of the wetting phase. The approximative analysis only gives a crude picture of the (a) to (b) transition, since n_c jumps from 1 to 0. As visible in Fig. 3, the ϵ location of this transition is shifted by roughly 20%, since the surface tension of the AB interface is overestimated. The (b) to (d) transition, on the other hand, is well described by the analysis and the partial densities are in good quantitative agreement with the simulation data. Thus the approximative analysis gives a qualitatively correct picture of the phase separation scenario and even predicts the (b) to (d) phase separation line quantitatively.

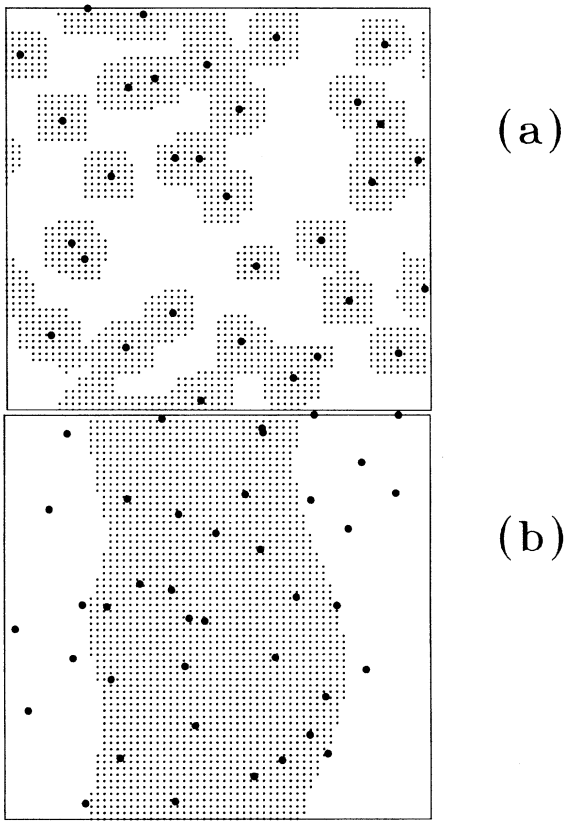

FIG. 2. Colloid positions (black circles) projected from a slab to the xy plane of the simulation box. The height of the slab in z direction is one-third of the total box height. The dark pixels whose resolution corresponds to the finite grid in the xy plane indicate that the z average of $\phi(\mathbf{r})$ is positive (region of phase A). The parameters are $\rho = 0.382\sigma^{-3}$, $\alpha = 4$, and $\epsilon = 0.1$. Clustered situation (a) ($G = 4$, $\xi = 0.05\sigma$, $f_0 = 2k_BT/\sigma^3$, and $E = 2$). Phase-separated situation (b) ($G = 0.1$, $\xi = 0.2\sigma$, $f_0 = 2.5k_BT/\sigma^3$, and $E = 1$).

In conclusion, depending on the microscopic parameters, phase separation can either spontaneously occur from a situation where only one solvent phase is involved or from clusters of the wetting phase A around the colloidal particles. A topological diagnosis of this phase reveals that the phase-A clusters are nonpercolating, containing few colloidal particles near phase separation. Phase separation in the colloidal fluid is thus directly connected to a percolation transition of the wetting solvent phase.

We finish with four remarks: First, the solvent-induced phase separation is driven energetically. It thus differs from the demixing transition due to a depletion zone of added polymer [16] or solvent [17] around the colloidal

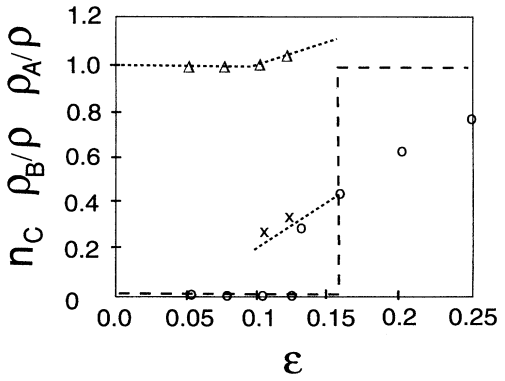

FIG. 3. Computer simulation results for the averaged number of phase-A clusters per particle, n_c (circles) and the partial densities ρ_A/ρ (triangles) and ρ_B/ρ (crosses) versus ϵ. The parameters are as in Fig. 1 with $\gamma = 0.5k_BT/\sigma^2$. The dashed lines are the corresponding results of the approximative analysis.

particles which is purely driven by entropy. Second, our theory does not apply close to a solvent critical point, since critical fluctuations which may give rise to attractive Casimir forces between the particles [18] are neglected in our mean-field model. Third, the Ginzburg-Landau approach can be extended to long-ranged order-parameter interactions as well as to a situation where the flocculated colloidal phase A is crystalline. Results along these lines will be published elsewhere [19]. Last, a rapidly increasing number of experimental investigations on colloidal suspensions have been performed using real-space methods. The advantage compared to static light scattering used in previous experiments [4] is that the topological properties of the clustered fluid phase are accessible by resolving the spatial regions of the different solvent phases. It would be interesting to verify the predicted percolation character of the (a) to (b) transition directly in real space.

[1] T. des Coudres, referred to in L. Rhumbler, Wilhelm Roux Arch. Entwicklungsmech. Organ. **7**, 225 (1898).

[2] For a brief historical review, see E. A. Boucher, J. Chem. Soc. Faraday Trans. I **85**, 2963 (1989).

[3] P. A. Albertsson, *Partition of Cell Particles and Macromolecules* (Wiley-Interscience, New York, 1986), 3rd ed.; *Aqueous Two-Phase Systems,* edited by H. Walter and G. Johansson, Methods in Enzymology Vol. 228 (Academic Press, San Diego, 1994).

[4] D. Beysens and D. Estéve, Phys. Rev. Lett. **54**, 2123 (1985); V. Gurfein, D. Beysens, and F. Perrot, Phys. Rev. A **40**, 2543 (1989); J. S. van Duijneveldt and D. Beysens, J. Chem. Phys. **94**, 5222 (1991); T. Narayanan, A. Kumar, E. S. R. Gopal, D. Beysens, P. Guenoun, and G. Zalczer, Phys. Rev. E **48**, 1989 (1993).

[5] P. D. Gallagher and J. V. Maher, Phys. Rev. A **46**, 2012 (1992).

[6] P. N. Pusey, in *Liquids, Freezing and the Glass Transition,* edited by J. P. Hansen, D. Levesque, and J. Zinn-Justin (North-Holland, Amsterdam, 1991).

[7] D. Beysens, J. M. Petit, T. Narayanan, A. Kumar, and M. L. Broide, Ber. Bunsen-ges. Phys. Chem. **98**, 382 (1994).

[8] S. Dietrich, in *Phase Transitions and Critical Phenomena,* edited by C. Domb and J. Lebowitz (Academic Press, London, 1987), Vol. 12, p. 1.

[9] F. Brochard and P. G. de Gennes, Ferroelectrics **30**, 33 (1980); T. Vilgis, A. Sans, and G. Jannink, J. Phys. II (France) **3**, 1779 (1993).

[10] For a review, see R. Evans, Adv. Phys. **28**, 143 (1979); H. Löwen, Phys. Rep. **237**, 249 (1994).

[11] M is a fictitious quantity since we are only interested in static averages.

[12] J. P. Hansen and I. R. McDonald, *Theory of Simple Liquids* (Academic Press, London, 1986), 2nd ed.

[13] R. Car and M. Parrinello, Phys. Rev. Lett. **55**, 2471 (1985).

[14] H. Löwen, P. A. Madden, and J. P. Hansen, Phys. Rev. Lett. **68**, 1081 (1992).

[15] J. P. Hansen, Phys. Rev. A **2**, 221 (1970).

[16] S. Asakura and F. Oosawa, J. Chem. Phys. **22**, 1255 (1954); E. J. Meijer and D. Frenkel, Phys. Rev. Lett. **67**, 1110 (1991).

[17] T. Biben and J. P. Hansen, Phys. Rev. Lett. **66**, 2215 (1991); M. Dijkstra and D. Frenkel, Phys. Rev. Lett. **72**, 298 (1994).

[18] M. Krech, *The Casimir Effect in Critical Systems* (World Scientific, Singapore, 1994).

[19] H. Löwen, Z. Physik B (to be published).

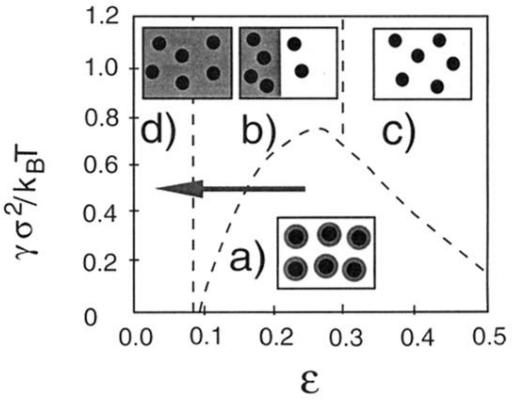

FIG. 1. Region of stability of the situations (a)–(d) in $\epsilon\gamma$ plane separated by the dashed lines as obtained within the approximate analysis. The parameters are $\rho = 0.382\sigma^{-3}$, $G = 10$, $f_0 = 2k_BT/\sigma^3$, $E = 30$, and $\alpha = 11.1$. The arrow corresponds to the path shown in Fig. 3. The colloid positions (black circles) and the grey region of phase A are schematically given in each situation.